# FORTE Observations of Simultaneous VHF and Optical Emissions from Lightning: Basic Phenomenology

D. M. Suszcynsky

M. W. Kirkland

A. R. Jacobson

R. C. Franz

S. O. Knox

*Los Alamos National Laboratory,*

*Space & Atmospheric Sciences Group, MS D466*

*Los Alamos, NM 87545*

J. L. L. Guillen

J. L. Green

*Sandia National Laboratories*

*Sensors and Electronics Dept., MS 0972*

*Albuquerque, NM 87185*

## ABSTRACT

Preliminary observations of simultaneous VHF and optical emissions from lightning as seen by the FORTE spacecraft are presented. VHF/optical waveform pairs are routinely collected both as individual lightning events and as sequences of events associated with cloud-to-ground (CG) and intra-cloud (IC) flashes. CG pulses can be distinguished from IC pulses based on the properties of the VHF and optical waveforms, but mostly based on the associated VHF

spectrograms. The VHF spectrograms are very similar to previous ground-based HF and VHF observations of lightning and show signatures associated with return strokes, stepped and dart leaders, attachment processes, and intra-cloud activity. For a typical IC flash, the FORTE-detected VHF is generally characterized by impulsive broadband bursts of emission and the associated optical emissions are often highly structured. For a typical initial return stroke, the FORTE-detected VHF is generated by the stepped leader, the attachment process, and the actual return stroke. For a typical subsequent return stroke, the FORTE-detected VHF is mainly generated by dart leader processes. The detected optical signal in both return stroke cases is primarily produced by the in-cloud portion of the discharge and lags the arrival of the corresponding VHF emissions at the satellite by a mean value of 243 μs. This delay is comprised of a transit time delay (mean of 105 μs) as the return stroke current propagates from the attachment point up into the region of in-cloud activity plus an additional delay due to the scattering of light during its traversal through the clouds. The broadening of the light pulse during its propagation through the clouds is measured and used to infer a mean of this scattering delay of about 138 μs (41 km additional path length) for CG light. This value for the mean scattering delay is consistent with the *Thomason and Krider*, [1982] model for light propagation through clouds. The dual phenomenology nature of these observations is discussed in terms of its ability to contribute to a satellite-based lightning monitoring mission.

## 1. INTRODUCTION

Space-based observations of lightning and thunderstorms in both the radio frequency (e.g. *Herman et al*., [1965]; *Holden et al*., [1995]; *Horner and Bent*, [1969]; *Kotaki and Katoh*, [1983]; *Leiphart et al*., [1962]; *Massey and Holden*, [1995]) and optical (e.g. *Sparrow and Ney*, [1971]; *Turman*, [1978]; *Vonnegut et al*., [1983]; *Vorpahl et al*., [1970]) parts of the electromagnetic spectrum have been made since the 1960s (see also the review by *Goodman and Christian* [1993]). However, apart from a few brief experiments using the Global

Positioning System's Nuclear Detonation System (GPS/NDS) in the 1990s, and limited use of a fast photodiode in conjunction with the BLACKBEARD very high frequency (VHF) radio experiment aboard the ALEXIS satellite (e.g. *Holden et al*., [1995]), no specifically designed space-based efforts have been mounted to simultaneously observe optical and radio frequency (RF) emissions from lightning on a routine, automated basis. The importance of performing such a study is clear. A dual phenomenology approach to lightning observations from space might significantly contribute to our eventual ability to monitor and remotely identify lightning types (cloud-to-ground, intra-cloud, etc.) from satellites. This has significant implications for planned NASA missions to eventually monitor lightning activity from geosynchronous orbit (*Goodman et al*., [1988]; *Christian et al.*, [1989]). In addition, dual RF/optical observations of lightning from satellites can also provide unique data sets from which to study the basic physics of lightning on a global scale.

In remedy of this situation, the Fast On-Orbit Recording of Transient Events (FORTE) satellite was launched on Aug. 29, 1997. FORTE is a joint Los Alamos National Laboratory and Sandia National Laboratories satellite experiment that was primarily designed to address technology issues associated with treaty verification and the monitoring of nuclear tests from space. The satellite carries VHF broadband radio receivers and an Optical Lightning System (OLS) that are optimally designed for the detection of lightning transients. The design of this instrumentation and its availability for continuous scientific use make FORTE an ideal space platform from which to monitor and study the simultaneous emission of VHF and optical radiation from lightning.

This paper reports on the preliminary phenomenology and analysis of the correlated FORTE VHF and optical data sets. The goals of this study are two-fold: (1) to demonstrate the utility of using a dual phenomenology approach for the remote identification of lightning types from space (cloud-to-ground versus intra-cloud), and (2) to use the unique perspective of the

FORTE data set to study basic lightning emission processes, the effects of clouds on the propagation of light transients, and general lightning phenomenology at the global level.

The paper is organized as follows. Following the introduction in section 1, section 2 provides a brief description of the instrumentation used for the study. The experimental results are described in section 3. Section 3a presents the basic phenomenology of simultaneous VHF and optical emissions from lightning as observed by FORTE. Examples of cloud-to-ground (CG) and intra-cloud (IC) flashes are shown. Section 3b defines what is meant by correlation time, scattering delay, and physical delay and details the technique that was used to measure/estimate each quantity. Measurements of these quantities using a 237-event study set are presented as histograms. Section 3c presents the results of an effort to estimate the rate of occurrence of detecting VHF/optical waveform pairs. Finally, section 4 discusses the results of section 3 with an emphasis on comparisons to models and previous results.

**2. INSTRUMENTATION**

FORTE is situated in a nearly circular, 70°-inclination orbit of approximately 825-km altitude with an orbital period of about 100 minutes. The instrumentation used for this study includes the two narrower-band FORTE VHF receivers as described in *Jacobson et al.*, [1998], and the Photodiode Detector (PDD) of the FORTE OLS which is described in *Kirkland et al.*, [1998].

The VHF instrumentation consists of two broadband receivers that can each be independently configured to cover a 22-MHz sub-band in the 30 - 300 MHz frequency range. For this study, one receiver was chosen to span the 26 - 48 MHz range and the other spanned the 118 - 140 MHz range. The instruments were configured to collect 40960 samples in a 800 μs record length resulting in a time resolution of 20 ns (sample rate of 50 MSa/s). The trigger point in each record allowed for 500 μs of pre-trigger information and 300 μs of post-trigger

information. The record length and pre/post trigger intervals were chosen to optimize the detection and identification of the VHF lightning emissions. Data collection is triggered off the lower (26 - 48 MHz) band receiver when the amplitude of its detected signal exceeds a preset noise-riding amplitude threshold in at least five of eight 1-MHz wide sub-bands distributed throughout the 22-MHz bandwidth (*Jacobson et al.*, [1998]). This triggering technique allows the instrument to trigger on and detect weak lightning signatures in the presence of strong interfering manmade carriers. Retriggering can occur after only a few microsecond delay allowing the instrument to record extended multi-record signals with essentially zero dead-time. The "field-of-view" of the VHF receivers is determined by the antenna pattern; the 3-dB attenuation contour of the antenna response approximates a circle of about 1200 km diameter and was chosen to roughly correspond to the 80° field-of-view of the PDD.

The PDD is a broadband (0.4 - 1.1 μm) silicon photodiode detector that collects amplitude versus time waveforms of lightning transients. The instrument has an 80° field-of-view which translates into a footprint of about 1200-km diameter for an 825-km altitude orbit. The instrument is typically configured to produce 1.92 ms records with 15 μs time resolution. The PDD is typically amplitude-threshold triggered, with a noise-riding threshold, and with a requirement that the signal exceed the amplitude threshold for five consecutive samples before a trigger occurs. This protocol eliminates false triggers due to energetic particles. However, the instrument can also be slaved to the VHF receivers whereby a trigger is forced whenever a VHF signal is received. The PDD provides 12-bit sampling with a piece-wise linear dynamic range covering four orders of magnitude and a sensitivity of better than $10^{-5}$ $W/m^2$. Several background compensation modes allow the instrument to be operated both at night and at a reduced sensitivity in the day. There is also a minimum inter-trigger delay of about 4.4 ms which results in a ~2.5 ms minimum dead time between successive records. The trigger times of both the VHF and PDD records are GPS-time-stamped to a 1 μs precision.

## 4. OBSERVATIONS AND ANALYSIS TECHNIQUES

### 3a. Basic VHF/Optical phenomenology

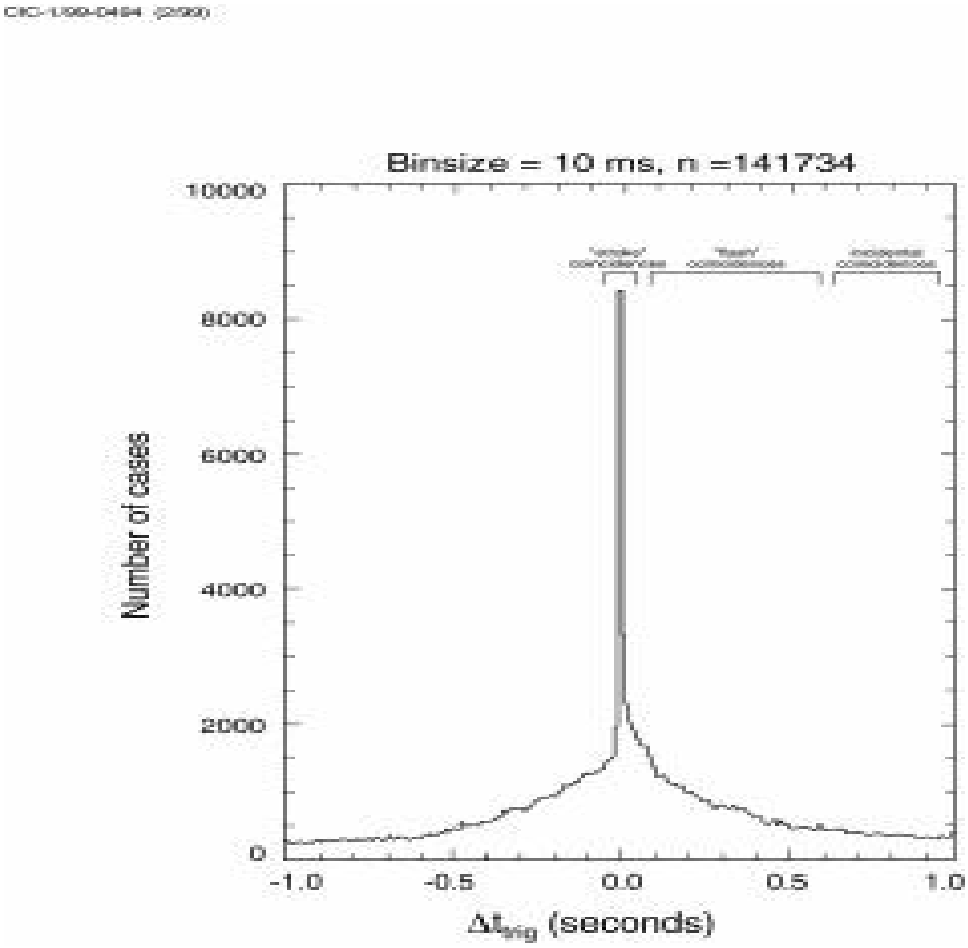


Figure 1 contains a histogram of the trigger time differences (i.e. approximate coincidence times), $\Delta t_{trig}$, between 141734 VHF and optical data records that were collected in the September 5, 1997 to April 15, 1998 time period. The VHF receivers and the PDD were operated autonomously during this period, so the coincidence rate between the VHF and optical triggers was heavily dependent upon the triggering and sensitivity biases of each particular instrument. Nonetheless, a robust collection of time coincidences is apparent. Three classes of coincidences are seen in Figure 1: (1) a narrow and statistically significant population of time coincidences at $\Delta t_{trig} \sim 0$ s represents correlations between near-simultaneous emissions of VHF and optical radiation from the same lightning pulse (here, the

term “pulse” refers to an individual stroke or feature in a multi-stroke cloud-to-ground (CG) flash, or an individual pulse of radiation from an intra-cloud (IC) flash made up of many pulses), (2) a broad population of time coincidences in the $0 < |\Delta t_{trig}| < 0.5$ s time interval that generally represents correlations between the VHF emissions associated with one pulse in a flash and the optical emissions from another pulse in that same flash, and (3) incidental time coincidences in the $|\Delta t_{trig}| > 0.5$ s regions that are not physically related. For the remainder of the paper, we will only consider coincidences (correlations) of the first type in which the VHF and optical radiations are presumably emitted from the same physical event ($\Delta t_{trig} \sim 0$ s).

An inspection of typical individual correlation cases ( Figures 2 and 3) confirms the above interpretation of Figure 1 and demonstrates the basic phenomenology of the VHF/optical correlations.

Figure 2a shows a sequence of four consecutive PDD triggers that occur over a 0.25 s time interval. The vertical spikes are actual PDD waveforms that appear compressed because of the large time scale displayed. The red triangles mark the reported times of three strokes of a three-stroke negative CG flash as identified by National Lightning Detection Network (NLDN) data. Figure 2b shows a corresponding sequence of three consecutive VHF waveforms that were collected over the same time interval. As can be seen, the FORTE data set captures the majority of the VHF and optical pulses emitted from the NLDN-reported CG flash. Figures 2cde present the detailed comparison of the three VHF/optical pairs in the flash. The VHF waveforms are displayed on an arbitrary amplitude scale to facilitate time comparisons with the optical waveforms. In each case the VHF signal is seen to precede the optical signal by tens to a few hundreds of microseconds, depending on how the time delay is measured. Figures 2fgh show the VHF spectrograms for the three VHF records displayed in

Figures 2cde. The spectrograms were generated by taking 256-sample Blackman-windowed fast fourier transforms of the waveform as the window was moved in 16-sample increments through the record. The spectrograms plot the signal power expressed in dBm (color bar) as a function of frequency and time and show features that are uniquely characteristic of CGs (see Section 4). The arrows in Figures 2fh indicate the NLDN-reported stroke times. The times are corrected for propagation delays to the satellite by using the NLDN source locations, the satellite location, and the WGS84 ellipsoid model of the Earth.

The data is also populated with examples of likely IC flashes, although the NLDN array is generally not useful in validating these examples because of its relative insensitivity to discharges which have predominantly horizontal currents. Instead, we identify candidate IC flashes by searching for time intervals (~ 1 - 10 ms) between successive triggers that are characteristic of IC activity.

Figure 3 shows an example of a likely IC flash in the same format as Figure 2. Note the 1 - 10 ms intervals between successive pulses. As with the CG example, the VHF signal precedes the optical signal by tens to hundreds of microseconds and the VHF spectrograms show features that are uniquely characteristic of ICs (see Section 4).

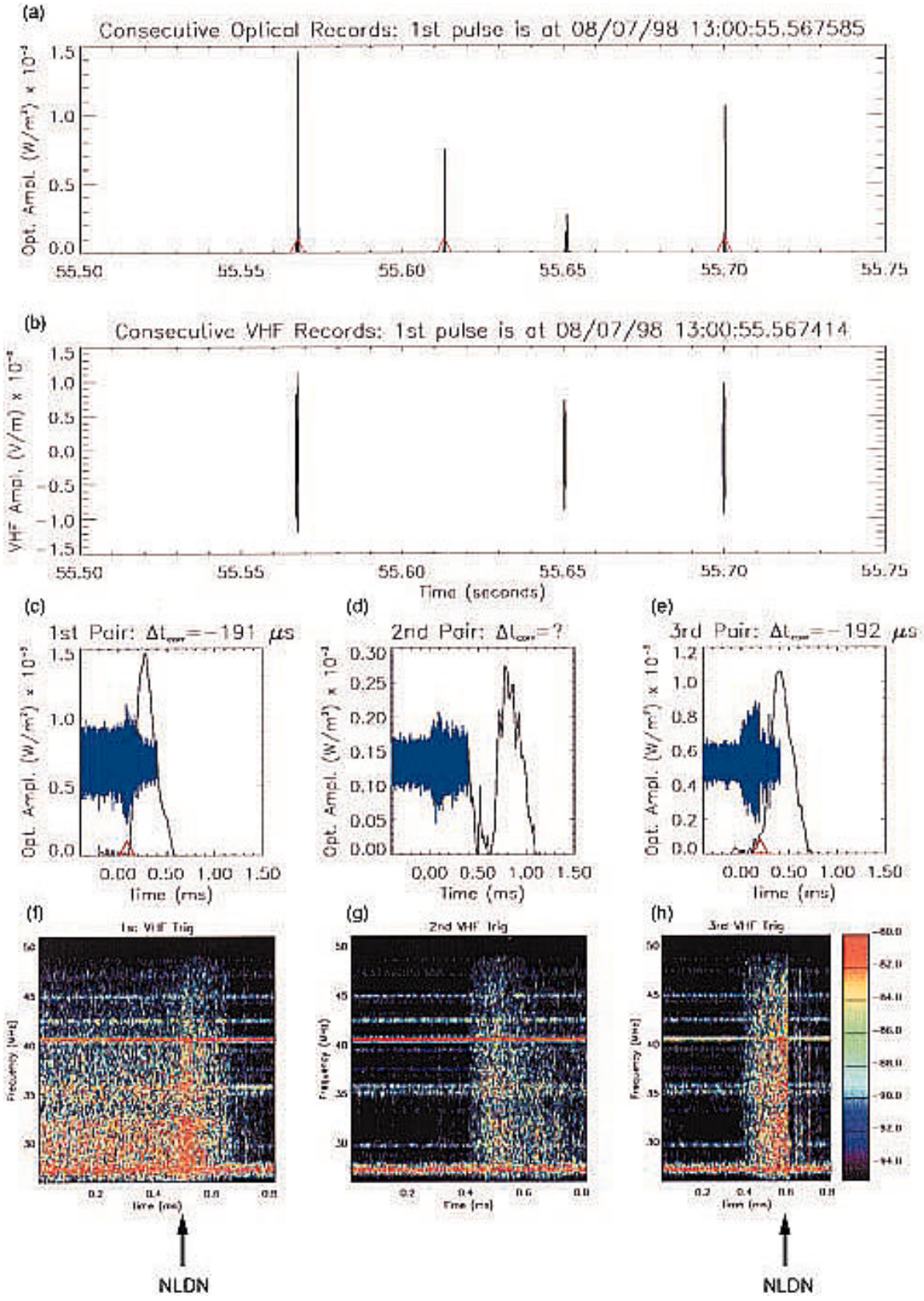
(a)
Consecutive Optical Records: 1st pulse is at 08/07/98 13:00:55.567585
Opt. Ampl. (W/m²) x 10⁻⁴
55.50
55.55
55.60
55.65
55.70
55.75
(b)
Consecutive VHF Records: 1st pulse is at 08/07/98 13:00:55.567414
VHF Ampl. (V/m) x 10⁻⁴
Time (seconds)
(c)
1st Pair: Δt = −191 μs
(d)
2nd Pair: Δt = ?
(e)
3rd Pair: Δt = −192 μs
Opt. Ampl. (W/m²) x 10⁻⁴
Time (ms)
(f)
(g)
(h)
Frequency (MHz)
NLDN
NLDN

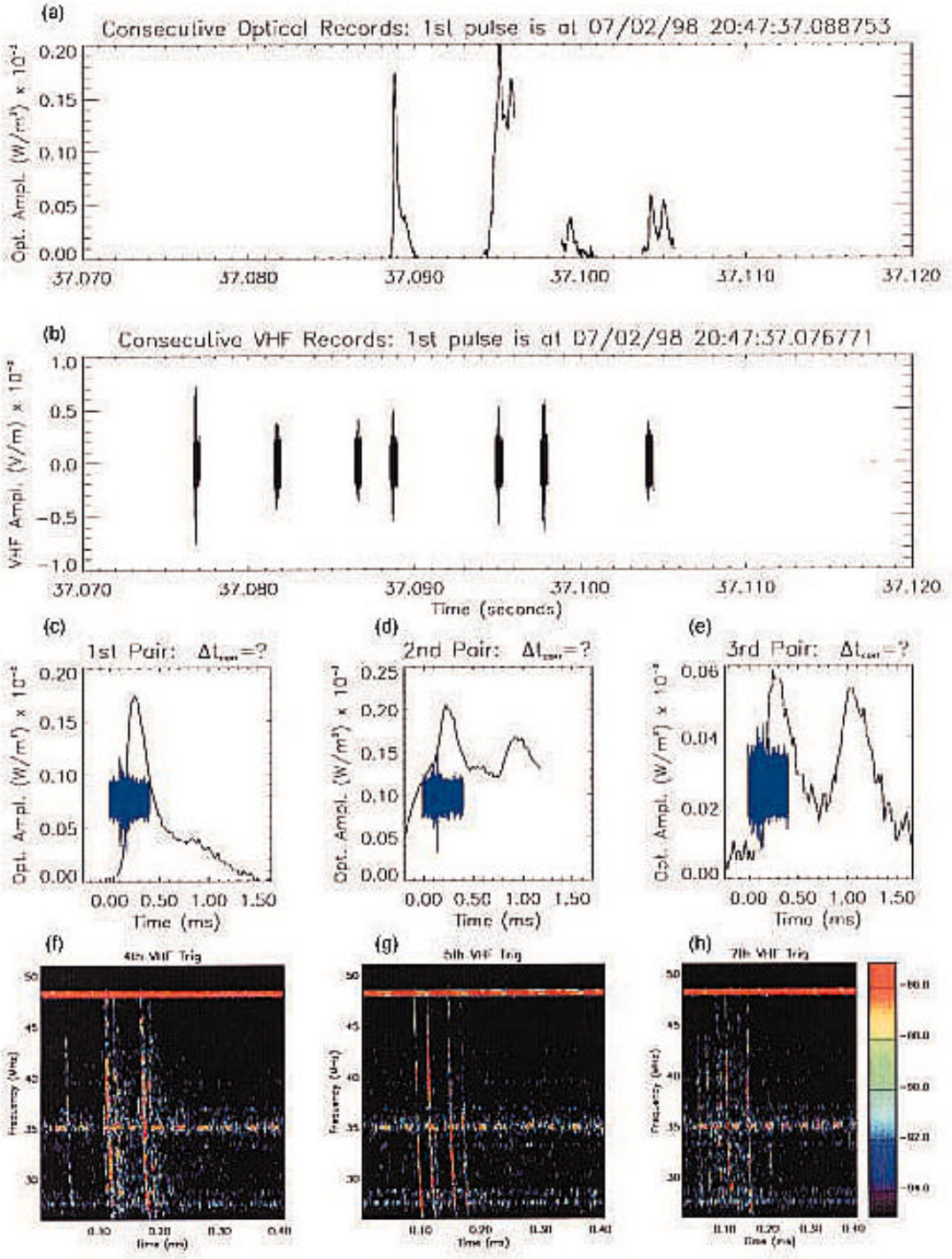
(a)
Consecutive Optical Records: 1st pulse is at 07/02/98 20:47:37.088753
Opt. Ampl. (W/m²) x 10⁻²
0.20
0.15
0.10
0.05
0.00
37.070
37.080
37.090
37.100
37.110
37.120
(b)
Consecutive VHF Records: 1st pulse is at 07/02/98 20:47:37.076771
VHF Ampl. (V/m) x 10⁻²
1.0
0.5
0.0
−0.5
−1.0
37.070
37.080
37.090
37.100
37.110
37.120
Time (seconds)
(c)
1st Pair: Δt = ?
Opt. Ampl. (W/m²) x 10⁻²
0.20
0.15
0.10
0.05
0.00
0.00 0.50 1.00 1.50
Time (ms)
(d)
2nd Pair: Δt = ?
Opt. Ampl. (W/m²) x 10⁻²
0.25
0.20
0.15
0.10
0.05
0.00
0.00 0.50 1.00 1.50
Time (ms)
(e)
3rd Pair: Δt = ?
Opt. Ampl. (W/m²) x 10⁻²
0.06
0.04
0.02
0.00
0.00 0.50 1.00 1.50
Time (ms)
(f)
(g)
(h)

### 3b. Correlation time, scattering delay, and physical delay: Definition and measurement

The degree to which the VHF signal precedes the optical signal is an important parameter to measure since the delay in the arrival of the optical signal at the satellite can be related to the scattering delay of light as it propagates through the clouds (e.g. *Thomason and Krider*, [1982]). An experimental determination of this number can be used to validate existing light propagation models but is complicated by the fact that the delays may also be influenced by whether or not the observed VHF and optical emissions are both emitted by the same process in the lightning discharge. Unless ground truth is available, it can be difficult to assess this contribution to the total delay. As a first step in deducing the optical scattering delay due to clouds, a subset of VHF/optical correlation data was analyzed to remove the triggering and thresholding biases that are introduced by considering trigger time differences (as in Figure 1) rather than true signal arrival time differences (i.e. correlation times). Because of the complex and variable nature of both the VHF and optical waveforms (see Figures 2 and 3), the true correlation times, $\Delta t_{corr}$, were analyzed and measured by hand, a laborious process that resulted in a much more limited, but more physically meaningful, data set.

Figure 4 illustrates how the correlation times, $\Delta t_{corr}$, were defined, measured, and related to the scattering delay, $\Delta t_{scatt}$. We assume that for a generic lightning pulse of radiation (e.g. an individual step in a stepped leader, a return stroke in a flash, a dart leader, etc.), the VHF emission from the source (driven by changes in current, dI/dt) will precede the emission of light (driven by current, I) by a time no greater than on the order of the risetime of the current pulse (about 1-10 μs). This assumption is supported by numerous field experiments (e.g. *Guo and Krider*, [1982]; *Ganesh et al.*, [1984]; *Beasley et al.*, [1983]; *Mach and Rust*, [1993]) and laboratory simulations of lightning discharges (e.g. *Gomes and Cooray*, [1998]). In addition, we must allow for any additional physical delay, $\Delta t_{phys}$, between the FORTE-

detected VHF emission and the FORTE-detected optical emission that would result if the VHF is emitted from one stage of the discharge and the optical emission is emitted from another stage.

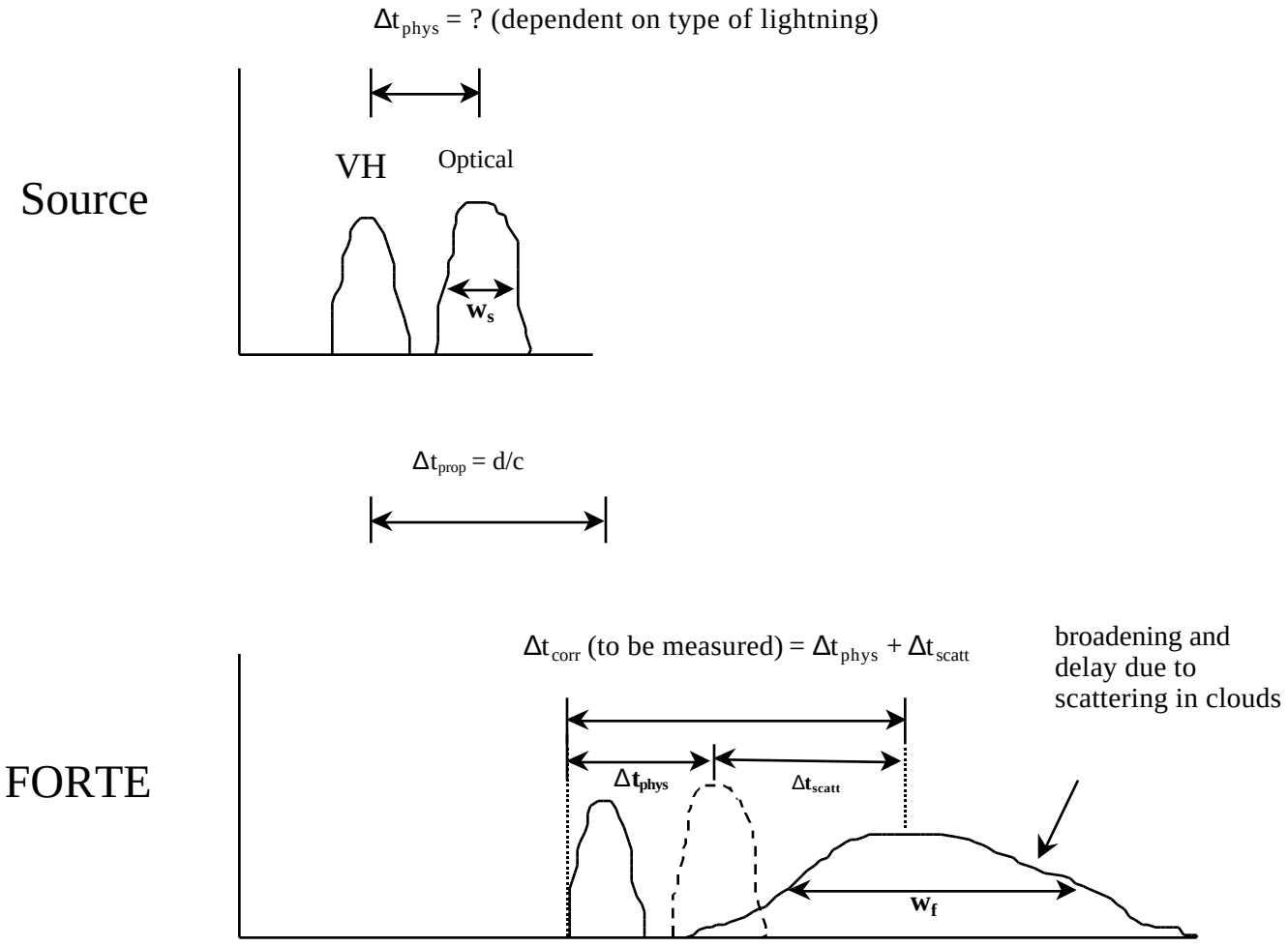

For example, interferometer observations of the VHF emitted around the time of first return strokes often show that the strongest VHF emissions occur near the time of the attachment process (e.g. *Shao et al*., [1995]). On the other hand, modeling results for the propagation of optical lightning transients to a satellite (e.g. *Thomason and Krider*, [1982]) indicate that the light emitted from the in-cloud portion of a CG discharge will reach a satellite relatively un-attenuated as compared to the below-cloud portion of the CG flash. In this case then, one might expect the PDD to detect just the in-cloud portion of the discharge and consequently, the entire event would exhibit a $\Delta t_{phys}$ on the order of the transit time of the return stroke current from the attachment point to the in-cloud region, or about 100 μs [e.g. see *Uman*, [1987]).

So, depending on what the sources of the radiations are, $\Delta t_{phys}$ may have a value of anywhere from a few microseconds (for cases where the detected VHF and optical signals are emitted from the same stage of the discharge) up to tens and hundreds of microseconds (for cases where the detected radiations are emitted from different stages of a discharge). Both radiations then propagate to the satellite with a time delay given by $\Delta t_{prop} = d/c$ where d is the source-satellite distance and c is the speed of light. However, the optical signal will acquire an additional delay, $\Delta t_{scatt}$, as well as a broadening, both due to the significant Mie scattering that occurs during the light's propagation through the clouds.

$\Delta t_{scatt}$ as well as an estimate for $\Delta t_{phys}$ can be determined by making two measurements. The first is the "delay measurement" where the time difference of arrival between the VHF signal and the optical signal at the satellite, $\Delta t_{corr}$, is measured and equated to the sum of $\Delta t_{phys}$ and $\Delta t_{scatt}$. For return strokes, $\Delta t_{corr}$ was determined by measuring the interval between the onset of the return stroke, as determined by the VHF spectrograms and/or NLDN data, and the peak of the associated optical pulse. For IC pulses, $\Delta t_{corr}$ was determined by measuring the interval between the onset of the impulsive VHF, as determined by the VHF spectrograms

and/or NLDN data, and the peak of the associated optical pulse. This method introduces an inherent uncertainty in the measured delay on the order of the risetime of the current pulse (1 -10 μs), but this is small compared to the measured $\Delta t_{corr}$ values. These measurement points were chosen because they correspond to features in both the VHF and optical records that are unambiguously identifiable and physically meaningful.

The second measurement is the "broadening measurement" where the broadening of the pulse, or difference between the pulse width at FORTE versus that at the source, $w_F - w_s$, is directly equated to $\Delta t_{scatt}$. The convention for measuring the width of an optical pulse is to integrate the full optical waveform over time and then divide by the peak irradiance to arrive at an effective pulse width (*Mackerras et al.*, [1973]). In this manner, $w_F$ is measured from the PDD waveforms and $w_s$ is estimated from ground-based measurements of CG activity below the cloud level. Implicit in this technique, is the assumption that the broadening of the light pulse due to scattering is equal to the time delay of the light pulse due to scattering. This assumption is valid as long as the PDD waveforms and the distribution function for the scattering delay of photons propagating through the cloud are fairly symmetric and single-peaked. Both of these requirements are generally met.

The analysis procedure for a given VHF/optical waveform pair, then, is summarized as follows: (1) determine $\Delta t_{scatt}$ by measuring the amount of optical pulse broadening, (2) measure $\Delta t_{corr}$ as described above, (3) then subtract $\Delta t_{scatt}$ from $\Delta t_{corr}$ to also arrive at an estimate for $\Delta t_{phys}$ that can be used to confirm the spectrogram interpretation.

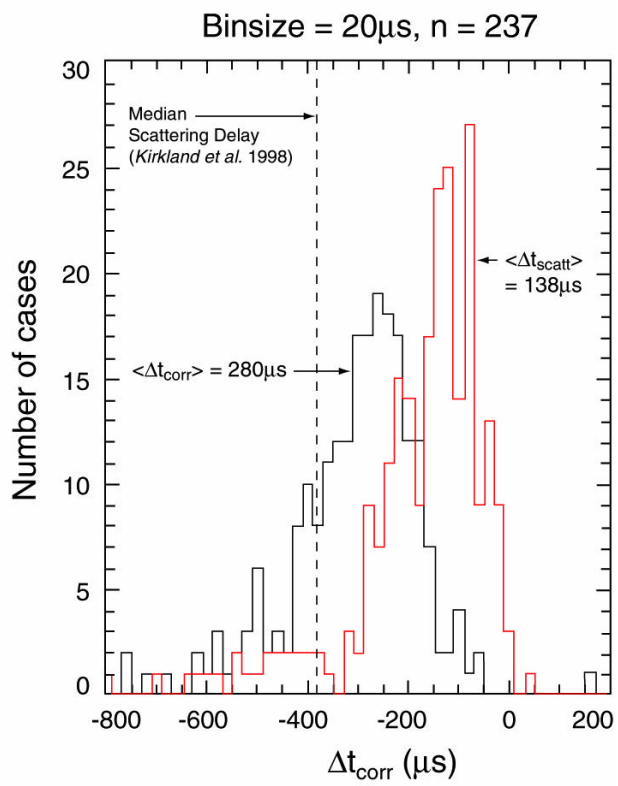


Figure 5 shows a histogram of $\Delta t_{corr}$ as measured with the above technique for a collection of VHF/optical waveform pairs. The pairs were randomly selected from a three week period of data collecting over the continental United States and bordering regions and include the observation of well over 40 storms. VHF record lengths of 800 μs with 500 μs of pre-trigger time were used to assure that the VHF triggers were of isolated events and not just one small interval of a more extensive emission. The uncertainty in each measurement of $\Delta t_{corr}$ is estimated to be about +/- 50 μs and reflects uncertainties in the optical time-tagging and in properly identifying the start of the return stroke and the peak of the associated optical signal. Of the 264 cases studied, 237 had unambiguous waveforms that allowed $\Delta t_{corr}$ to be directly measured with the described technique. The 27 ambiguous cases consisted of 14 IC pulses and 13 unidentified pulses and were not measured. $\Delta t_{corr}$ values of IC events are generally not measurable because of the difficulty in making a one-to-one correspondence between the complex VHF spectrogram features (see Figures 3fgh) and the optical waveform features. The mean value of the 237 measured $\Delta t_{corr}$ 's was -243 μs where the minus sign indicates that the VHF signal preceded the arrival of the optical signal at the satellite.

Examples of individual $\Delta t_{corr}$ measurements for return strokes can be seen in Figure 2. The measured $\Delta t_{corr}$ 's for each of the three VHF/optical pairs are indicated on the tops of Figures 2cde. In keeping with measurement convention, a $\Delta t_{corr}$ for the VHF/optical pair shown in

Figure 2d was not measured since the optical peak is ambiguous. The NLDN-reported return stroke onset times are indicated by the arrows below Figures 2fh. The peak times of the optical signals are obvious and not marked. An important observation concerning the 237 measured cases is that 225 (131 confirmed by NLDN and 94 inferred from the spectrogram patterns) were associated with CGs. Of the remaining 12 cases, nine were associated with TIPP's (*Holden et al.*, [1995]; *Massey and Holden*, [1995]; *Jacobson et al.*, [1998]) and three were associated with IC pulses.

Figure 5 also contains a second histogram (red line) that shows the results of the broadening measurement. In order to compare this result with the $\Delta t_{corr}$ measurements, we calculated the effective pulse width for the 237 cases as described above, subtracted 200 μs which represents an estimated average effective pulse width for CGs at the source based on the ground measurements of *Mackerras et al.*, [1973] *and Guo and Krider*, [1982], and then took the negative of each result in order to facilitate comparison with the $\Delta t_{corr}$ histogram. The resulting histogram produces a $<\Delta t_{scatt}>$ (i.e. mean broadening) of about 138 μs, which equates to a 41 km additional photon path length. We can then calculate $< \Delta t_{phys}>$ as $< \Delta t_{phys}> = <\Delta t_{corr}> - <\Delta t_{scatt}> =$ 243 μs - 138 μs 105 μs. This value of $< \Delta t_{phys}>$ indicates that on the average, there is a 105 μs delay at the source region between the emission of the VHF radiation that is detected by FORTE and the emission of the optical radiation that is detected by FORTE.

**3c. VHF/Optical Correlations: Rate of Occurrence**

Finally, experiments were performed to estimate the rate of occurrence of detecting simultaneous VHF/optical triggers from lightning events. An estimate of the rate of correlation between the VHF and optical signals has a bearing on the future use of dual phenomenology (VHF plus optical) sensors to execute a satellite-based lightning monitoring mission. With both instruments operating autonomously, as for the data in Figure 1,

approximately 0.2 % of the collected VHF lightning events are accompanied by a correlated optical lightning signal, and about 0.4 % of the optical lightning events are associated with a correlated VHF lightning signal. These correlation rates are fairly low and result from the fact that each instrument operates independent of the other and is biased by its own triggering and thresholding schemes. Indeed, in the course of normal operations, the instruments are typically configured to minimize false alarms at the expense of not detecting the weakest signals.

A controlled experiment was performed to measure a more meaningful occurrence rate by running the PDD in the slave mode, effectively removing all PDD triggering biases. Data was collected over a four-day period by forcing a PDD trigger whenever the VHF receivers triggered on a lightning event. It was found that 722 VHF lightning triggers out of a total of 6342 events were accompanied by a correlated optical lightning signature giving an occurrence rate of 11.4 %, almost two orders of magnitude greater than when the instruments were operated autonomously. The nighttime rate was even greater (606 out of 3258 events for a 21.8% correlation rate) and is a result of the higher sensitivity of the PDD in nighttime conditions. These numbers represent a lower limit to the occurrence rate for correlations since the effective field-of-view of the VHF receivers is significantly larger than that of the PDD.

## 4. DISCUSSION

### 4a. Basic VHF/Optical Phenomenology.

The identification of the various lightning features in Figures 2 and 3 is somewhat speculative since adequate ground truth, specifically in the form of radiation waveforms with the proper time resolution, is lacking. The NLDN data offers some ground truth on return strokes although it must be kept in mind that NLDN does not provide waveforms and employs an LF/VLF magnetic field direction-finding system as opposed to the FORTE receivers which

measure broadband VHF radiation. No optical ground truth was available for the study. An additional consideration for the detection of CG VHF is that the look direction for the FORTE sensors is generally parallel to the channel current flow while that of ground-based measurements is generally perpendicular. Consequently, any directionality in lightning VHF emissions might result in significantly different signatures observed by FORTE as opposed to ground measurements. Despite these limitations, the routine association of certain FORTE VHF signatures with certain types of NLDN-verified activity, as is shown in Figure 2, provides us with a good degree of confidence in tentatively assigning interpretations to the features in the spectrograms. This confidence is further supported by striking similarities between the FORTE VHF data and previous ground-based measurements and identifications of HF and VHF emissions from various phases of CG activity (e.g. *Levine and Krider*, [1977]; *Hayenga*, [1984]; *Rhodes et al*., [1994]; *Shao et al*., [1995], *Mazur et al*., [1995]).

Figures 2fgh and 3fgh contain spectrogram patterns that are typical for those associated with CG and IC flashes. The final interpretation of these types of spectrograms depended upon an iterative approach, culminating when a self-consistent analysis was attained between the FORTE VHF and optical observations, the corresponding NLDN data, and the bibliography of previous ground-based interferometer measurements. In the remainder of this subsection, we detail the unique identifying characteristics of each type of lightning displayed in Figures 2 and 3.

The broadband signal in the first 500 μs of the spectrogram in Figure 2f (initial return stroke) is tentatively identified as stepped leader emission. The leader emission is immediately followed by an additional 100 μs burst of radiation that is most likely associated with the actual propagation of the return stroke current. Unlike subsequent strokes, initial return strokes are typically characterized by VHF emissions during the actual return stroke process, presumably related to the characteristic branching of first return stroke channels (e.g. *Levine*

*and Krider*, [1977]). The attachment process presumably occurs at the temporal boundary between the stepped leader and the return stroke. Although not obvious in Figure 2f, the time of attachment is often characterized by an intense, narrow (~ a few μs) burst of VHF such as that shown by the arrow in the example of Figure 6.

In order to correctly relate the VHF emission to the detected optical emission for first return strokes in the format of Figure 4, we make the assumption that the detected optical signal is associated with the return stroke process and that any optical emissions related to the stepped leader are generally too weak to be detected. This assumption is vindicated, for example, by the above-cloud aircraft measurements of *Goodman et al.*, [1988] in which optical emissions from stepped leaders were rarely measured.

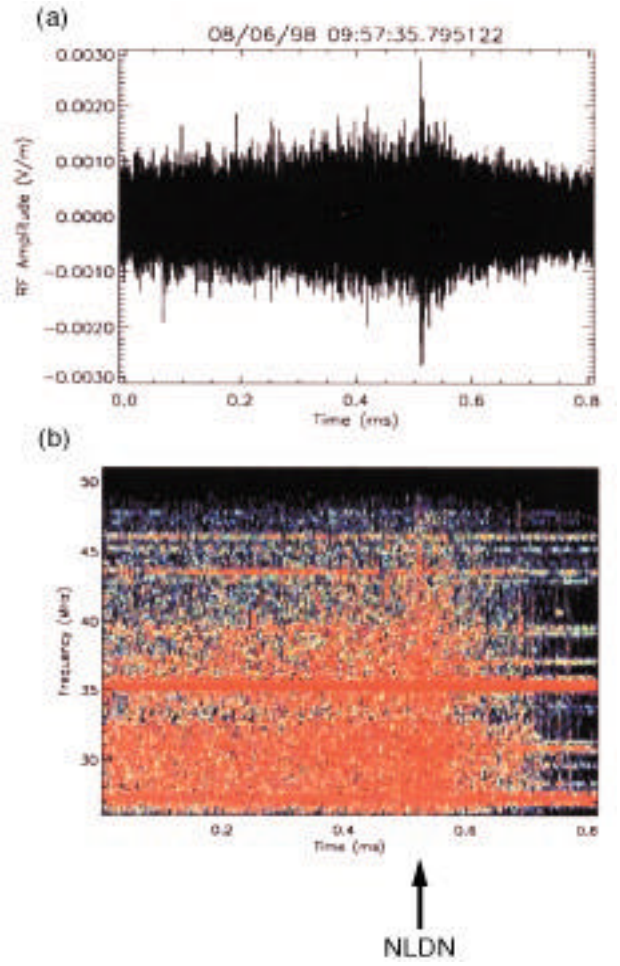

In summary, the above identification of first return stroke features is supported by the following observations: (1) the NLDN detection of the onset of the return stroke occurs at the end of the purported leader emission and at the beginning of the burst associated with the return stroke as expected, (2) ground-based interferometer measurements of first return strokes show similar features that agree with those in Figure 2f in terms of the relative intensity and timing of the strokes (e.g. *Rhodes et al*., [1994]; *Shao et al*., [1995]), (3) the time durations of the purported leader (always greater than 500 μs) and return stroke emissions ( ~ 100 μs) are consistent with those measured on the ground, (4) VHF emission is detected during the actual return stroke, and (5) as will be seen below, the measured $\Delta t_{corr}$, $\Delta t_{scatt}$ and $\Delta t_{phys}$ are consistent with the feature identification.

The two spectrograms shown in Figures 2gh are typical of subsequent strokes and display an initial interval where the VHF increases in intensity followed by either a steady decrease in intensity (Figures 2dg) or a more common sudden turn-off of emission (Figures 2eh) in coincidence with the onset of the return stroke. The time duration of the entire VHF emission associated with subsequent strokes is typically 100 - 400 μs. In both spectrograms, we identify the entire signal as due to dart leader emission. The gradual turn-off of radiation in Figures 2dg is currently unexplained and is further discussed later in this subsection. In summary, the above identification of subsequent return stroke features is supported by the following observations: (1) the NLDN detection of the onset of the subsequent return stroke occurs at the end of the purported dart leader emission as expected, (2) ground-based interferometer measurements of subsequent return strokes show similar features that agree with those in Figures 2gh in terms of relative intensity and timing (e.g. *Rhodes et al*., [1994]; *Shao et al*., [1995]), (3) the time durations of the purported dart leader are consistent with those measured on the ground, (4) the cessation of radiation at the onset of the subsequent return stroke is in agreement with ground measurements, and (5) as will be seen below, the measured $\Delta t_{corr}$, $\Delta t_{scatt}$ and $\Delta t_{phys}$ are consistent with the feature identification.

The interpretation of subsequent return stroke/dart leader spectrograms (Figures 2gh) is somewhat more difficult than that for initial strokes since their spectrogram signatures are slightly more variable. Dart leaders are strong VHF emitters (e.g. *Hayenga,* [1979]*; Levine and Krider*, [1977]; *Rhodes et al*., [1994]; *Shao et al*., [1995]) and are known to have a significant optical output that is typically on the order of 10 % of that associated with the parent return stroke (*Idone and Orville*, [1985]). Such a signal may be detectable by the PDD but at a much reduced amplitude as compared to the optical emission associated with the actual return stroke current. If optical dart leader signatures were in fact detected by the PDD, they would be temporally isolated from the main optical peak associated with the return stroke and easily identified (*Brook et al*., [1985]). However, nearly all of the optical signatures studied in this paper were single-peaked. Consequently, in order to correctly relate the detected VHF emission to the detected optical emission for subsequent strokes in the format of Figure 4, we assume that the dart leader optical emission does not significantly contribute to the overall signal detected by the PDD. This assumption is again supported by the measurements of *Goodman et al.*, [1988].

The degree to which FORTE detects the various strokes in the flash of Figure 2 is typical of the VHF/optical data set. All three NLDN-reported strokes are accompanied by PDD triggers while only two of the three strokes registered a VHF trigger. On the other hand, there is a fourth pulse at 55.65 s that was reported by both the VHF and PDD instruments, but wasn't reported by NLDN. This may simply be a stroke that was missed by the NLDN, or possibly an emission due to a K-event associated with the flash. K-events (or K-changes) often occur in IC flashes and as in-cloud events between successive strokes in a multi-stroke CG flash and can produce significant optical and VHF radiation ( e.g. see the review by *Rakov et al.,* [1992]). Indeed, *Goodman et al.*, [1988] reported above-cloud observations of K-event optical intensities associated with CGs that exceeded those associated with the return strokes.

K-events between return stroke intervals have been equated to dart leaders that do not propagate to ground and have VHF signatures that are similar to those associated with subsequent return strokes (e.g. *Rhodes et al*., [1994]; *Shao et al*., [1995]). Consequently, it is likely that some of the "subsequent strokes" that are included in Figure 5 and that are identified by their VHF spectrograms rather than by NLDN data are, in fact, between-stroke K-events/aborted leaders. It is possible that the VHF/optical pair at 55.65 s is due to a K-event. This might explain why, unlike Figure 2h, there is no sharp cutoff in the VHF emission of Figure 2g. However, at this point, such an identification is pure speculation since we currently have no way to confirm K-events in the FORTE data set.

The impulsive nature of the VHF spectrogram signals for IC pulses (Figure 3fgh) is presumably related to short multiple bursts of current and is a characteristic signature of FORTE-detected IC pulses (see also *Jacobson et al*., [1999]). These signals are TIPP-like ( *Holden et al*., [1995]; *Massey and Holden*, [1995]; *Jacobson et al*., [1998]) in that they are impulsive and are separated by tens of microseconds. However, unlike TIPPS, they occur in multiple pairs, several pairs often occurring within one 800 μs record. Analogously, the optical waveforms for IC pulses are often more structured than those associated with CG strokes. Given the impulsive, multiple nature of the IC VHF signals seen in Figures 3fgh, we interpret this optical structure to be the result of closely spaced individual optical pulses that are broadened and coalesced by scattering.

The near absence of IC VHF/optical waveform pairs for the data in Figure 5 is unexplained. Again, it is possible that some of the "subsequent strokes" in Figure 5 are actually due to IC K-events. But even with this potential misidentification, it is still clear that CGs dominate the data in Figure 5. Given the fact that IC flashes are much more common than CG flashes (*Prentice and Mackerras*, [1977]; *Mackerras et al*., [1998]), this would seem to indicate that the FORTE detection of VHF/optical pairs of waveforms is preferential to CGs. This is in

contrast to the result that we find when the FORTE VHF and optical data sets considered individually (*Jacobson et al*., [1999]; *Suszcynsky et al*, [1999]). In each of these cases, IC detections are more numerous than CG detections. A full analysis and explanation of this observation necessitates a comparison between VHF and PDD triggering biases, source current waveforms and VHF/optical signal risetimes for CG versus IC pulses and is beyond the scope of this paper.

A more detailed analysis that quantifies the VHF spectrograms and optical signal characteristics for specific types of lightning is ongoing and will be reported on in a subsequent paper. However, it is already clear from this initial analysis that an analysis of VHF signatures of lightning in tandem with optical data can greatly enhance a satellite's ability to discriminate lightning types from space. Some discrimination information can be found in the optical waveforms: for example, IC waveforms are often broader and more structured than CG waveforms. However, the bulk of the discrimination capability in the FORTE instruments seems to lie in the interpretation of the VHF spectrograms. Based on the 131 NLDN-corroborated cases from the data shown in Figure 5, we find that we can distinguish between initial return strokes, subsequent return strokes and intra-cloud discharges at a better than 90% confidence level.

**4b. $<\Delta t_{corr}>$, $<\Delta t_{scatt}>$, and $<\Delta t_{phys}>$.**

The value for $<\Delta t_{phys}>$ that was deduced from the measurements in Figure 5 can be compared to previous experimental data. Ground-based interferometer measurements indicate that the strongest VHF near the time of initial return strokes occurs during the attachment process and that this emission typically precedes the in-cloud portion of the return stroke by ~ 100 μs (e.g. *Shao et al*, [1995]). Our measurement of $<\Delta t_{phys}> = 105$ μs is in good agreement with this time delay. Likewise, for subsequent strokes, the measured $<\Delta t_{phys}>$ is comparable in value to the time delay expected between the initiation of the subsequent return stroke and

the optical in-cloud activity that follows. These comparisons imply that the FORTE-detected VHF from CGs is generally produced by below-cloud processes (leaders, attachment processes, and in the case of initial strokes, the actual return stroke) while the FORTE-detected light from CGs is produced by the in-cloud portion of the return stroke. The implication is that, in general, return stroke light emissions originating below the cloud deck are reflected and scattered to the extent that they fall below the detection threshold of the PDD.

It is important to emphasize that these last two statements have been formulated only for the type of data that we are analyzing in this paper, i.e. for lightning events in which *both* VHF and optical signals are collected. For example, when looking at only optical/NLDN correlations we sometimes find what appear to be examples of optical emissions from stepped leaders, dart leaders, and below-cloud portions of return strokes. However, these examples are relatively uncommon. Also, when looking at only VHF/NLDN correlations, the dominant lightning events are TIPPs rather than CGs (*Jacobson et al*., [1999]).

A comparison between the measured $<\Delta t_{scatt}>$ and predictions from various cloud scattering models is generally difficult since the initial conditions of the models do not always match up to the existing conditions during the FORTE measurements. Likewise, the existing cloud and source conditions during the FORTE measurements are not well understood, particularly in the absence of ground truth. However, the measured $<\Delta t_{scatt}>$ of 138 $\mu$s compares favorably to the results of *Thomason and Krider*, [1982]. The *Thomason and Krider*, [1982] model for light propagation through clouds is based on a Monte Carlo method that simulates Mie scattering processes driven by homogenous clouds of various dimensions and particle-size compositions. The model is particularly applicable to the FORTE data set since it considers light scattering and absorption of impulsive point source emissions placed at various locations within finite, geometric clouds. For a light transient located at the center of a cubic cloud of

optical depth 200 and water drop diameter of 10 μm (moderate maritime cumulonimbus), the model predicts a $<\Delta t_{scatt}>$ of about 51 μs (15 km increased path length) while the predicted value for an optical depth of 400 (strong maritime cumulonimbus) is 130 μs (39 km increased path length). The $<\Delta t_{scatt}>$ result of Figure 5 compares only generally to the recent measurements of *Philsticker et al.,* [1998] that show a scattering delay on the order of 350 μs for two observed cumulonimbus thunderstorm clouds of 5 km vertical extent. These values were measured for transmission of light from a source above the clouds (the sun) to the detector below the clouds and tend to significantly overestimate the additional path length that one would expect for a source near the center of the cloud, as would be the case for IC lightning or the in-cloud components of return strokes.

*Kirkland et al*., [1998] used the full FORTE/PDD data set to estimate a $<\Delta t_{scatt}>$ value greater than 447 μs (114 km). Since the *Kirkland et al*., [1998] width distribution was non-normal, their median value of $\Delta t_{scatt}$ = 380 μs is the more appropriate value to use for comparisons to this study. This value is marked as a vertical dashed line in Figure 5 and is significantly greater than the $<\Delta t_{scatt}>$ value shown in the histogram of Figure 5. The discrepancy between the *Kirkland et al.,* [1998] result and the result of this study is apparently a function of lightning type. *Kirkland et al*. [1998] did not distinguish between CG and IC-produced light. Since IC pulses are the predominant type of lightning and since the IC light signals detected by FORTE are generally broader and more structured than those associated with CGs, the inclusion of IC light in the *Kirkland et al*, [1998] statistics tends to bias the estimate for $<\Delta t_{scatt}>$ to larger values than those associated with just CGs. In fact, when the *Kirkland et al*. [1998] analysis was reapplied to just CG events (4424 NLDN-confirmed cases (*Suszcynsky et al*., [1999])), we calculated a mean effective pulse width of approximately 203 μs, much closer to the 138 μs value measured for this study.

In conclusion, satellite-based collection of simultaneous VHF and optical emissions from lightning transients is a powerful technique that can be used to study both thunderstorm and lightning processes on a global basis. The preliminary results of this study indicate that we can use VHF/optical correlations to (1) effectively identify and distinguish between CG and IC pulses, including stepped and dart leaders, attachment processes, and return strokes, and (2) estimate a mean scattering delay for the in-cloud portion of CG-emitted light (138 μs).

**ACKNOWLEDGEMENTS**

The authors would like to thank Paul Kreihbel of The New Mexico Institute of Mining and Technology, and Paul Argo, Anthony Davis, Dott Delapp, Bob Roussel-Dupre, Diane Roussel-Dupre, Ken Eack, Dan Holden, Phil Klingner, Charley Rhodes, Xiaun-Min Shao, and Dave Smith of Los Alamos National Laboratory for useful discussions, comments, and support during this study. This work was supported by the United States Department of Energy.

**REFERENCES**

Beasley, W. H., M. A. Uman, D. M. Jordan, and C. Ganesh, Simultaneous pulses in light and electric field from stepped leaders near ground level, *J. Geophys. Res., 88,* 8617-8619, 1983.

Brook, M., C. Rhodes, O. H. Vaughan, Jr., R. E. Orville, and B. Vonnegut, Nighttime observations of thunderstorm electrical activity from a high altitude airplane, *J. Geophys. Res., 90,* 6111-6120, 1985.

Christian, H. J., R. J. Blakeslee**,** and S. J. Goodman, The detection of lightning from geostationary orbit, *J. Geophys. Res., 91,* 13329-13337, 1989.

Ganesh, C., M. A. Uman, W. H. Beasley, and D. M. Jordan, Correlated optical and electric field signals produced by lightning return strokes, *J. Geophys. Res., 89*, 4905-4909, 1984.

Gomes, C., and V. Cooray, Correlation between the optical signatures and current waveforms of long sparks: applications in lightning research, *J. Electrost., 43*, 267-274, 1998.

Goodman, S. J., H. J. Christian, and W. D. Rust, A comparison of the optical pulse characteristics of intracloud and cloud-to-ground lightning as observed above clouds, *J. Applied Meteor., 27*, 1369-1381, 1988.

Goodman, S. J. and H. J. Christian, Global Observations of Lightning, in Atlas of Satellite Observations Related to Global Change, 1993.

Guo, C. and E. P. Krider, The optical and radiation field signatures produced by lightning return strokes, *J. Geophys. Res., 87*, 8913-8922, 1982.

Hayenga, C. O., Characteristics of lightning VHF radiation near the time of the return stroke, *J. Geophys. Res., 89*, 1403-1410, 1984.

Herman, J. R., J. A. Caruso, and R. G. Stone, Radio astronomy explorer (RAE-1), observation of terrestrial radio noise, *Planet. Space Sci., 21*, 443-461, 1965.

Holden, D. N., C. P. Munson, and J. C. Devenport, Satellite observations of transionospheric pulse pairs, *Geophys. Res. Lett., 22(8)*, 889-892, 1995.

Horner, F. and R. B. Bent, Measurement of terrestrial radio noise, *Proc. Roy. Soc. A, 311*, 527-542, 1969.

Idone, V. P. and R. E. Orville, Correlated peak relative light intensity and peak current in triggered lightning subsequent return strokes, *J. Geophys. Res., 90*, 6159-6164, 1985.

Jacobson, A. R., S. O. Knox, R. Franz, D. C. Enemark, FORTE observations of lightning radio-frequency signatures: capabilities and basic results, submitted to *Radio Sci*., 1998.

Jacobson, A. R., K. L. Cummins, M. Carter, P. Klingner, D. Roussel-Dupre, S. O. Knox, FORTE observations of lightning radio-frequency signatures: Prompt coincidence with National Lightning Detection Network sferics, submitted to *J. Geophys. Res*., 1999.

Kirkland, M. W., D. M. Suszcynsky, R. Franz, J. L. L. Guillen, J. L. Green, Observations of terrestrial lightning at optical wavelengths by the photodiode detector on the FORTE satellite, submitted to *J. Geophys. Res*., 1998.

Kotaki, M. and C. Katoh, The global distribution of thunderstorm activity observed by the ionosphere sounding satellite (ISS-b), *J. Atmos. And Terr. Physics, 45*, 833-847, 1983.

Leiphart, J. P., R. W. Zeek, L. S. Bearce, and E. Toth, Penetration of the ionosphere by very low frequency radio signals. Interim results of the LOFTO-I experiment, *Proc. of the IRE, 6*, 6-17, 1962.

Levine, D. M. and E. P. Krider, The temporal structure of HF and VHF radiations during Florida lightning return strokes, Geophys. Res. Lett., 4, 13-16, 1977.

Mach, D. M., and W. D. Rust, Two-dimensional velocity, optical risetime, and peak current estimates for natural positive lightning return strokes, *J. Geophys. Res.*, *98*, 2635-2638, 1993.

Mackerras, D., Photoelectric observations of the light emitted by lightning flashes, *J. Atmos. Terr. Physics*, *35*, 521-535, 1973.

Mackerras, D., M. Darveniza, R. E. Orville, E. R. Williams, and S. Goodman, Global lightning:Total, cloud and ground flash estimates, *J. Geophys. Res.*, *103*, 19791-19809, 1998.

Massey, R. S. and D. N. Holden, Phenomenology of transionospheric pulsed pairs, *Radio Sci., 30(5)*, 1645-1659, 1995.

Mazur, V., P. R. Krehbiel, and X. M. Shao, Correlated high-speed video and radio interferometric observations of a cloud-to-ground lightning flash, *J. Geophys. Res.*, *100*, 25731-25753, 1995.

Pfeilsticker, K., F. Erle, O. Funk, L. Marquard, T. Wagner, and U. Platt, Optical path modifications due to tropospheric clouds: Implications for zenith sky measurements of stratospheric gases, *J. Geophys. Res., 103*, 25323-25335, 1998.

Prentice, S. A. and D. Mackerras, The ratio of cloud to cloud-ground lightning flashes I thunderstorms, *J. Appl. Meteorol.*, *16*, 545-550, 1977.

Rakov, V. A., R. Thottappillil, and M. A. Uman, Electric field pulses in K and M changes of lightning ground flashes, *J. Geophys. Res.*, *97*, 9935-9950, 1992.

Rhodes, C. T., X. M. Shao, P. R. Kreihbel, R. J. Thomas, and C. O. Hayenga, Observations of lightning phenomena using radio interferometry, *J. Geophys. Res., 99,* 13059-13082, 1994.

Shao, X. M., P. R. Krehbiel, R. J. Thomas, and W. Rison, Radio interferometric observations of cloud-to-ground lightning phenomena in Florida, *J. Geophys. Res., 100*, 2749-2783, 1995.

Sparrow, J. G. and E. P. Ney, Lightning observations by satellite, *Nature, 232*, 540-541, 1971.

Suszcynsky, D. M., M. Kirkland, P. Argo, R. Franz, A. Jacobson, S. Knox, J. Guillen, J. Green, R. Spalding, Thunderstorm and Lightning Studies Using the FORTE/OLS, in press, Proceedings of the Eleventh International Conference on Atmospheric Electricity, 1999.

Thomason, L. W. and E. P. Krider, The effects of clouds on the light produced by lightning, *J. Atmosph. Sci., 39*, 2051-2065, 1982.

Turman, B. N., Analysis of lightning data from the DMSP satellite, *J. Geophys. Res., 83*, 5019-5024, 1978.

Uman, M. A., The Lightning Discharge, Academic Press, Orlando, 1987.

Vonnegut, B., O. H. Vaughan, and M. Brook, Photographs of lightning from the space shuttle, *Bull. Amer. Met. Soc., 64*, 150-151, 1983.

Vorpahl, J. A., J. G. Sparrow, and E. P. Ney, Satellite observations of lightning, *Science, 169*, 860-862, 1970.

**FIGURE CAPTIONS**

Figure 1. Histogram of VHF/optical trigger time differences, $\Delta t_{trig}$, for 141734 events in the Sept. 5, 1997 to April 15, 1998 time interval.

Figure 2. Example of an NLDN-confirmed negative CG flash. (a) consecutive PDD waveforms collected over a 0.25 s time interval with NLDN-detected strokes identified by red triangles, (b) consecutive VHF waveforms collected over the same time interval as in (a), (cde) expanded plots of the three VHF/optical waveform pairs shown in (a) and (b), (fgh) frequency-time spectrograms of the three VHF waveforms shown in (cde). The arrows below the spectrograms indicate the NLDN-reported onset times of the return strokes.

Figure 3. Example of a likely IC flash. Presentation format is the same as that described in Figure 2.

Figure 4. Definition and measurement strategy for $\Delta t_{corr}$, $\Delta t_{phys}$ , and $\Delta t_{scatt}$.

Figure 5. Histograms of $\Delta t_{corr}$ (solid line) and $\Delta t_{scatt}$ (broken line) for 237 VHF/optical correlations. The vertical dotted line at -380 μs represents the median effective scattering delay as measured by *Kirkland et al.,* [1999].

Figure 6. a) Time waveform and (b) frequency-time spectrogram of an initial return stroke showing an impulsive emission at 500 μs (arrow) associated with an attachment process.